SCIENCE CHINA
Chemistry

• ARTICLES •

May 2014 Vol.57 No.5: 763–771
doi: 10.1007/s11426-013-4992-8

Recyclable polymer-based nano-hydrous manganese dioxide for highly efficient Tl(I) removal from water

PAN BingCai[1,2*], WAN ShunLi[1], ZHANG ShuJuan[1], GUO QingWei[3], XU ZhengCheng[3], LV Lu[1,2] & ZHANG WeiMing[1,2]

[1]*State Key Laboratory of Pollution Control and Resource Reuse, School of the Environment, Nanjing University, Nanjing 210023, China*
[2]*National Engineering Center for Organic Pollution Control and Resource Reuse (Suzhou Division), Suzhou High-Tech Institute of Nanjing University, Suzhou 215123, China*
[3]*South China Institute of Environmental Science, Ministry of Environmental Protection, Guangzhou 510655, China*

Received June 11, 2013; accepted August 27, 2013; published online October 31, 2013

Tl(I) in water even at a trace level is fatal to human beings and the ecosystem. Here we fabricated a new polymer-supported nanocomposite (HMO-001) for efficient Tl(I) removal by encapsulating nanosized hydrous manganese dioxide (HMO) within a polystyrene cation exchanger (D-001). The resultant HMO-001 exhibited more preferable removal of Tl(I) than D-001 and IRC-748, an iminodiacetic chelating polymer, particularly in the presence of competing Ca(II) ions at greater levels in solution. Such preference was ascribed to the Donnan membrane effect caused by D-001 as well as the specific interaction between Tl(I) and HMO. The adsorbed Tl(I) was partially oxidized into insoluble Tl(III) by HMO at acidic pH, while negligible oxidation was observed at circumneutral pH. The exhausted HMO-001 was amenable to efficient regeneration by binary NaOH-NaClO solution for at least 10-cycle batch runs without any significant capacity loss. Fixed-bed column test of Tl(I)-contained industrial effluent and natural water further validated that Tl(I) retention on HMO-001 resulted in a conspicuous concentration drop from 1.3 mg/L to a value lower than 0.14 mg/L (maximum concentration level for industrial effluent regulated by US EPA) and from 1–4 μg/L to a value lower than 0.1 μg/L (drinking water standard regulated by China Health Ministry), respectively.

manganese dioxide, nanocomposite, thallium, water treatment

1 Introduction

Thallium (Tl) is a rare but widely distributed element in the environmental media [1–4]. In water, Tl mainly exists in two oxidation states, Tl(I) and Tl(III). Tl(I) is more stable or forms more stable compounds [4, 5]. The solubility of thallous compounds is generally high so that monovalent thallium is readily transported through aqueous routes into the environment [6]. Being a highly toxic element comparable to lead, mercury and cadmium [7, 8], Tl is associated with a variety of adverse health effects including alopecia, psychic disturbance, acute ascending paralysis and cardiovascular effects [9–11]. Hence, stringent regulations have been set up to control its maximum contaminant level (MCL). USA EPA [12] set MCL of Tl in industrial effluent and drinking water as 0.14 and 0.002 mg/L, respectively. In China, its MCL in drinking water was set at a much lower level (0.0001 mg/L) [13].

To date, much less attention has been paid to Tl than to other toxic metals like lead, mercury and cadmium. This is partly because Tl contamination is not globally important as of now. Nevertheless, it may be grave enough in certain mining areas, for instance, in some southwest provinces of China [14]. In addition, with the increasing demand for thallium in the high-technology and future-technology fields, Tl is being recognized as a potential pollution source on a large scale in future [3]. Hence, it is still necessary to mini-

*Corresponding author (email: bcpan@nju.edu.cn)

mize the thallium levels in the environment on account of its high toxicity to the public health. US EPA [12] recommended activated alumina and ion exchange as the best available techniques for Tl elimination from water. Unfortunately, efficient Tl removal from contaminated waters is still a challenging task for both processes, particularly in the presence of other co-ions (like Na^+, K^+, Ca^{2+}, and Mg^{2+}) at much greater levels. This is because all these co-ions will pose great competitive effect on Tl binding to activated alumina and ion exchangers, resulting in a low capacity and unacceptable cost. Recently, selective adsorption exhibits its great potential for efficient Tl removal, and some nanomaterials (e.g., nano-Al_2O_3) [15] or composite adsorbents like polyacryamide-aluminosilicate composites [16] were developed for this purpose. Yantasee *et al*. [17] fabricated two specific adsorbents, superpara-magnetic Fe_3O_4 nanoparticles modified by dimercaptosuccinic acid (DMSA) and mesoporous silica functionalized by copper ferrocyanide [18], and revealed their selective Tl sequestration in the presence of competing co-ions. Nevertheless, few adsorbents are available for efficient removal of Tl to meet the above-mentioned stringent regulations. Furthermore, no open literatures, to the best of our knowledge, are available concerning treatment of Tl-contaminated industrial effluents or natural waters based on selective adsorption.

In recent years, increasing polymer-based nanocomposite adsorbents have been developed for efficient treatment of water contaminated by various toxic metals, arsenic, and phosphate [19–22]. Such nanocomposite adsorbents usually consist of two sections, the charged polymeric beads of large size (usually around 1 mm in diameter for feasible separation or for excellent hydraulic properties) as the host and inorganic nanoparticles (e.g., hydrated ferric oxide [19, 20] or zirconium phosphate [23]) of specific affinity towards target pollutants, which are immobilized within the polymeric phase to prevent their aggregation and to improve their hydraulic properties. Moreover, suitable charged groups binding the polymeric hosts could favor the enrichment and permeation enhancement of trace target ionic pollutants based on Donnan membrane principle [19, 21]. However, the usability of polymeric nanocomposites for efficient Tl(I) removal from contaminated waters is unknown.

The primary objective of this study is to develop polymer-based nano-hydrous manganese oxide composite (HMO-001) and evaluate its efficiency for Tl(I) removal from waters. HMO-001 was obtained by encapsulating amorphous HMO nanoparticles within a commercially available polymeric cation exchanger D-001, and the negatively charged sulfonic acid groups being covalently bound to D-001 are expected to play a favorable role in Tl sequestration due to the potential Donnan membrane effect [19, 21]. Adsorption of Tl(I) instead of Tl(III) onto HMO-001 was examined because Tl(I) is usually the main Tl species in waters. The adsorption was evaluated in terms of effect of solution pH, competitive adsorption with co-ions, kinetics and column runs. As for column adsorption, Tl(I)-contaminated industrial effluents and natural waters were employed as the feeding solutions to test the feasibility of HMO-001 for practical application.

2 Experimental

2.1 Materials

All chemicals used in this study were of analytical grade or more pure and were purchased from Nanjing Zhongdong Station (Nanjing, China) except for $TlNO_3$, which was purchased from Aldrich-Sigma (China). The stock solution of 10 g/L Tl(I) was prepared by dissolving $TlNO_3$ in the deionized water. D-001, a polystyrene sulfone cation exchanger with the total exchange capacity of 4.30 meq/g, the cross-linking density of ~8%, and the bead with the diameter of 0.7–0.8 mm was purchased from Zhenguang Resin Co., China. Amberlite IRC-748, an iminodiacetic chelating resin widely used for selective metal capture in industry, was obtained from Rohm Haas Co. (USA). According to the information provided by the manufacture, the exchange capacity of IRC-748 is around 1.3–1.5 meq Na^+/g. Prior to use, both polymeric resins were subjected to rinsing with 1 mol/L HCl, 1 mol/L NaOH, and alcohol in sequence to remove possible impurities, followed by rinsing with deionized water. Both resins were converted to Na^+ form by flushing them in a fixed bed with 2 mol/L NaCl for 12 h. Prior to use, they were washed with deionized water and vacuum-desiccated at 333 K for 24 h until reaching a constant weight. The hydrous manganese oxide (HMO) particles were obtained according to the method proposed by Parida *et al*. [24].

2.2 Fabrication of HMO-001

HMO-001 was fabricated based on a propriety technique proposed by our research group [25]. In brief, the preparation of HMO-001 consists of the following steps: (1) 30.0 g of D-001 beads were added into 200 mL of 2.0 mol/L $MnCl_2$ solution, and then stirred continuously for 24 h to ensure Mn(II) loadings onto D-001 through electrostatic attraction; (2) the Mn(II)-loaded D-001 was added into a binary solution containing NaOH (10 w%) and NaOCl (active chlorine, 13%), where Mn(II) would be oxidized into hydrated Mn(IV) oxides (HMO) by NaOCl; (3) the HMO-impregnated polymeric beads were washed with 0.1 mol/L HCl and double-distilled water to neutralize the residual alkali, followed by desiccation under vacuum at 333 K for 12 h.

2.3 Batch adsorption and regeneration

A desired amount of adsorbent particles were introduced

into stoppered 250-mL Erlenmeyer flasks containing 100 mL solution of known Tl(I) concentration. Ca(II) was employed as a representative co-ion by introducing certain amounts of $Ca(NO_3)_2{\cdot}4H_2O$ into the test solution. A 1.0 mol/L HNO_3 or NaOH solution was used to adjust the solution pH throughout the experiment when necessary. The flasks were then transferred to a model G-25 incubator shaker with thermostat (New Brunswick Scientific Co. Inc.) and vibrated at 180 r/min for 24 h at a given temperature. Preliminary kinetic tests indicated that 24 h is enough to achieve adsorption equilibrium. For cyclic experiments the Tl(I)-laden sorbent particles were filtered and introduced into 5 mL solution containing NaOH (5 w%) and NaOCl (active chlorine, 7.8%). After 2 h the regenerated HMO-001 beads were filtered and rinsed with 5% NaCl solution and DI water until reaching neutral pH, and then employed for cyclic sorption runs. For the kinetic test, the initial solution volume was 1000 mL and aliquots of 1-mL were sampled at various time intervals. Note that all the batch runs were performed in duplicate for data analysis.

2.4 Fixed-bed column tests

Column adsorption experiments were carried out with a polyethylene column (12 mm in diameter and 130 mm in length) equipped with a water bath to maintain a constant temperature. Five milliliter of wet D-001 or HMO-001 particles was packed within two separate columns before operation. Except for synthetic feeding solutions containing Tl(I) and other components, TI(I)-contaminated industrial effluent from a mining plant in Guangdong Province (China) as well as natural waters near the mining plant were collected as the feeding solutions to test the feasibility of HMO-001 for practical application. Compositions of all the feeding solutions are described in the related figures. A Lange-580 pump (Baoding, China) was used to deliver the solutions at a constant flow rate. The hydrodynamic conditions for column sorption runs, i.e., a superficial liquid velocity (SLV) and an empty bed contact time (EBCT), are also presented in related figures.

2.5 Analyses

Tl(I) concentration was determined by atomic absorption spectroscope (Thermal Co. U.S.) and ICP-MS (ELAN9000, America), if lower than 1 mg/L. The detection limit of Tl(I) for AAS and ICP-MS is 0.5 mg/L and 0.01 μg/L, respectively. The appearances of D-001 and HMO-001 were displayed in two photographs. The loaded HMO on D-001 was ground for observation of a field-emission transmission electron microscope (Hitachi model H-800, Japan). The amount of HMO encapsulated within D-001 was determined by analyzing Mn content after digesting HMO-001 particles in a HNO_3-$HClO_4$ binary solution. Crystallinity of HMO inside the HMO-001 beads was determined by X-ray diffraction analysis with a step size of 0.02^o (XTRA, Switzerland). N_2 adsorption-desorption test onto both adsorbents were carried out at 77 K to determine pore size distribution based on BJH model by using Micromeritics ASAP2020 (U.S.). X-ray photoelectron spectroscope (XPS) analysis was performed on a PHI 5000 Versaprobe system, using monochromatic Al Kα radiation (1486.6 eV). All binding energies (BE) were referenced to the C1s peak at 284.6 eV.

3 Results and discussion

3.1 Characterization of HMO-001

HMO amount loaded within D-001 was determined as 9.5 (*w*/*w*)%. The successful loading of HMO was intuitively demonstrated by photographs of D-001 and HMO-001 (Figure 1(a) and (b)). TEM image of HMO-001 (Figure 1(c)) further indicated that HMO was capsulated within D-001 as nanoparticles or nanorods of size less than 20 nm, and the nanosized metal oxides usually possess larger accessible surface areas and stronger activities than the bulk ones [26, 27]. The X-ray diffraction pattern of the HMO-001 beads (Figure 1(d)) showed the presence of three weak and broad peaks at 25.06°, 37.16° and 66.12°, respectively. It is similar to those of the synthetic birnessite phase δ-MnO_2 [24, 28], indicating that most of the impregnated HMO was amorphous. The pore structure information presented in Table 1 suggests that HMO loading onto D-001 would cause an understandable drop of pore size and volume.

3.2 Effect of solution pH on Tl(I) adsorption

Effect of solution pH on Tl(I) uptake by HMO-001 as well as on the HMO leaching from HMO-001 was examined in the background solution of calcium ions as high as 20 mmol/L, and the results are depicted in Figure 2. As demonstrated earlier (data not shown), in this study 20 mmol/L calcium ions can sufficiently shield Tl(I) binding onto D-001 through nonspecific electrostatic interaction with the sulfonic groups. Thus, the pH-dependent adsorption edge could generally reflect its effect on Tl(I) binding by the immobilized HMO nanoparticles. The removal efficiency of Tl(I) decreased from ~75% to 52% with pH increase from 2 to 4, and then kept almost constant with a further increase even to 10.6. In addition, no HMO leaching was observed from HMO-001 when operated in pH higher than 3, and a slight HMO loss was observed in the pH range 2–3, indicating that HMO-001 can work well under weakly acidic or alkali solution. It is of practical merit because most of Tl(I)-contaminated industrial effluent or natural water are around neutral pH.

3.3 Effect of Ca^{2+} on Tl(I) adsorption

Here Ca^{2+} was selected as a representative competing ion

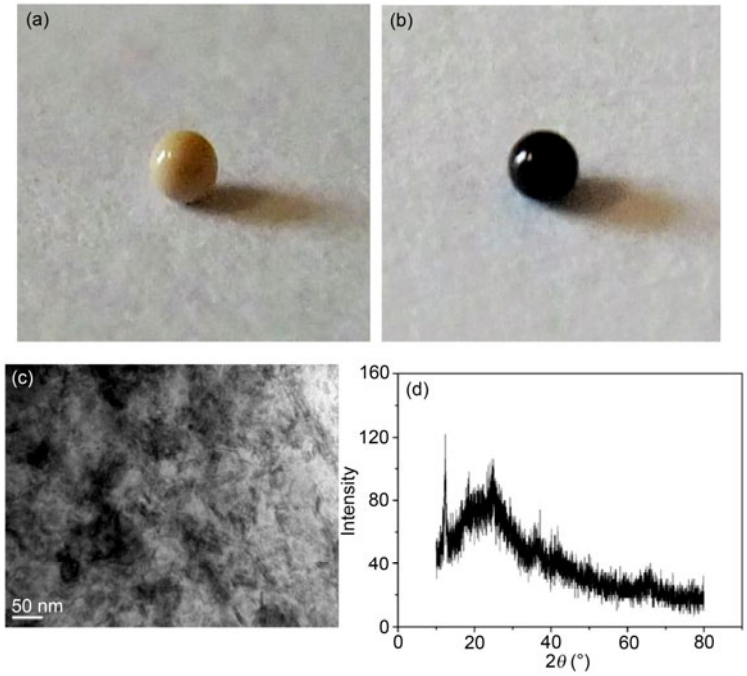

Figure 1 Characteristics of D-001 and HMO-001. (a) photo of D-001; (b) photo of HMO-001; (c) TEM of HMO-001; (d) XRD of HMO-001.

Table 1 Salient properties of the macroporous strong-acid cation exchanger D001 and its HMO-loaded derivative HMO-001

Designation	D-001	HMO-001
Matrix structure	Crosslinked polystyrene	
Functional group	$R–SO_3^-·Na^+$	
Pore volume (cm^3/g)	0.187	0.011
BET surface area (m^2/g)	16.21	4.95
Average pore diameter (nm)	16.25	3.93
Apparent density (g/mL)	1.09	1.37
HMO content (Mn %)	0	9.5

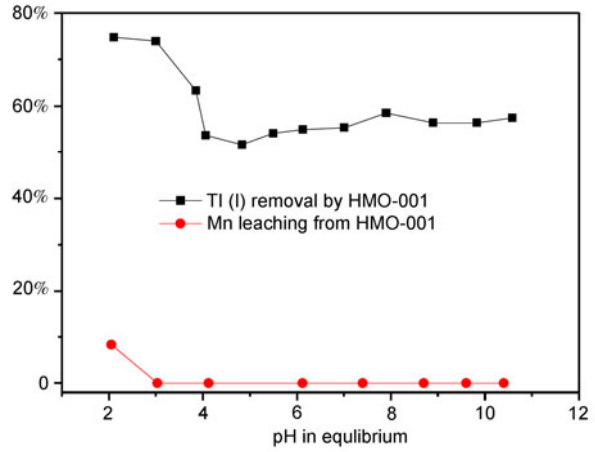

Figure 2 Effect of equilibrium solution pH on Tl(I) uptake onto HMO-001 and HMO leaching from HMO-001 at 298 K. S/L ratio = 1.00 g/L, initial Tl(I) 0.25 mmol/L and Ca(II) 20 mmol/L.

because it is usually more competitive than Na^+ or K^+ and Mg^{2+} [29], and its competitive effect on Tl(I) binding onto HMO-001 was evaluated. The host cation exchanger, D-001, and a metal-specific chelating resin, Amberlite IRC-748, were chosen as reference. As illustrated in Figure 3, Tl(I) adsorption by all the three sorbents were influenced by the Ca^{2+} addition to different contents. Tl(I) removal by D-001 was decreased dramatically from 100% to ~10% when increasing initial Ca^{2+}/Tl^+ ratio from 0 to 100. This is understandable because cation uptake onto D-001 is driven only by nonspecific electrostatic interaction, and the added Ca(II) ions will greatly compete for the binding sites of TI(I), i.e., the negatively charged sulfonic groups. As for Amberlite IRC-748, Tl(I) removal dropped down dramatically to near zero when the Ca^{2+}/Tl^+ molar ratio increased to 10, because Amberlite IRC-748 can selectively capture Ca(II) ions through the complexation with iminodiacetic groups. For HMO-001, however, it is a quite different case. Increasing initial Ca^{2+}/Tl^+ ratio from 0 to 20 results in an apparent decline of Tl(I) removal efficiency from ~100% to ~42%, and further increase in the Ca(II) ions even to 100 times of Tl(I) concentration does not impose any adverse effect on Tl(I) removal, indicating that HMO-001 exhibits preferable Tl(I) removal from the background solution of the competing Ca(II) ions even at much higher levels. In addition, a simple comparison between HMO-001 and activated alumina (Table S1) further suggested the potential of the former adsorbent for Tl removal.

3.4 Adsorption mechanism

On the basis of the structure of HMO-001, we assume that preferable Tl(I) adsorption onto HMO-001 is possibly ascribed to three aspects: (1) Donnan membrane effect caused

by the host resin D001. As known, Tl(I) adsorption onto D001 can be realized by coloumbic interaction and is a nonspecific process. However, the Donnan membrane effect of the polymeric exchangers, which has been clearly elucidated elsewhere [19, 21], is favorable for enhanced removal of target ions by HMO-001. In other words, the non-diffusible sulfonate groups binding D-001 would help enhance Tl(I) preconcentration and permeation within the polymeric phase prior to effective sequestration by nano-HMO. (2) Specific interaction between Tl(I) and nano-HMO. Various metal oxides like HMO interact specifically with toxic metal ions through the inner sphere complexation [30, 31]. Nevertheless, to the best of our knowledge, no literature is available concerning the possible inner sphere complexation between HMO and Tl(I). Here we just carried out a comparative study on Tl(I) adsorption by pure HMO particles and D-001. In fact, HMO exhibits more preferable adsorption towards Tl(l) than D001 (Figure 4), implying that HMO interacts with Tl(I) more specifically than the electrostatic attraction, though such specific interactions have not been clearly identified by the spectroscopic techniques like XAS. (3) Tl(I) oxidation into the insoluble Tl(III) species by HMO under acidic environment. We carried out an XPS analysis on Tl(I)-preloaded HMO-001 samples obtained at pH 2.2 and 5.8. The results described in Figure 5 suggested that around 52.6% of the adsorbed Tl(I) was oxidized into Tl(III) at pH 2.2, while that for pH 5.8 was only 3.9%. Correspondingly, at pH 2.2 Mn(IV) species decreased from 43.1% to 32.6%, and Mn(III) was increased from 45.0% to 55.9%. Nevertheless, at pH 5.8 no significant variation in Mn(IV) and Mn(III) species were observed. The above XPS results further indicated that at acidic pH (like 2.2 in this study) Tl(I) oxidation would contribute to its uptake by HMO-001, whereas at neutral pH (such as 5.8), the oxidation effect can be negligible on Tl(I) uptake. Note that around 3% of the encapsulated HMO was dissolved into solution at pH 2.2, whereas no Tl species were detected in solution. Such H^+-motivated oxidation of Tl(I) and precipitation onto manganese oxide has been reported by Bidoglio *et al*. [32], and the reduction of MnO_2 to Mn(III) or Mn(II) species requires the participation of protons [33]. For example, when the pH was decreased from 8.0 to 4.0, the reduction potential of MnO_2 was increased from 0.76 V to 0.99 V [34]. The formed insoluble Tl(III) species seems favorable for the release of the active adsorption sites for further Tl(I) sequestration, as demonstrated in the regeneration study.

3.5 Adsorption kinetics

The uptake of Tl(I) versus contact time for HMO-001 and D-001 were also studied and the results are depicted in Figure 6. As shown, initial adsorption was very quick, followed by a gradual adsorption approaching equilibrium within one hour. The pseudo-first-order kinetic model was employed to describe the sorption process [35]:

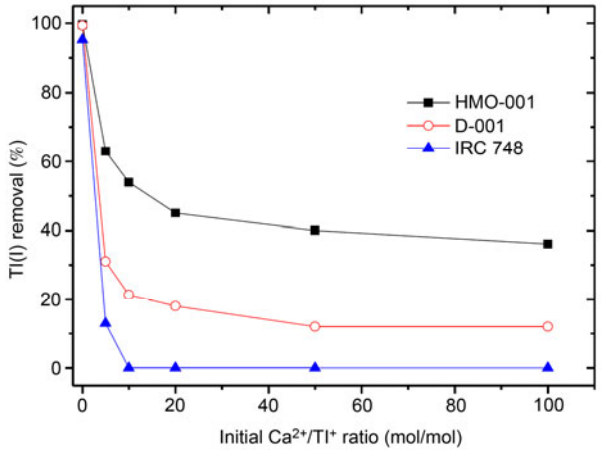

Figure 3 Effect of calcium ions on Tl(I) retention by HMO-001, D-001 and Amberlite IRC-748 at 298 K and initial pH 5.8. S/L ratio = 0.50 g/L, initial Tl(I) 0.25 mmol/L.

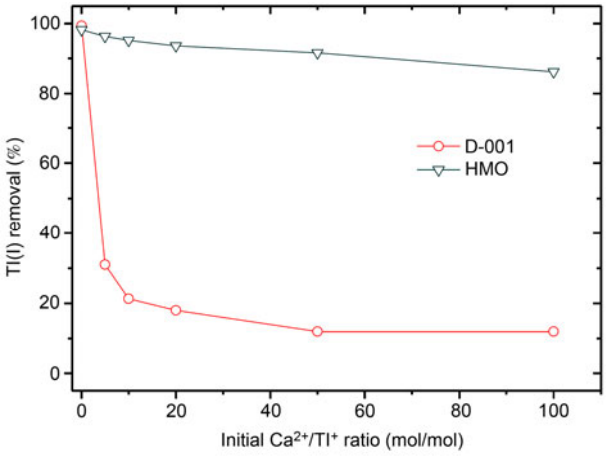

Figure 4 Effect of calcium ions on Tl(I) retention by HMO and D-001 at 298 K and pH 5.8. S/L ratio = 0.50 g/L, initial Tl(I) 0.25 mmol/L.

$$\log(q_e - q_t) = \log q_e - \frac{k_1}{2.303}t \quad (1)$$

where q_e and q_t are the amounts sorbed at equilibrium and at time t, respectively; k_1 is the first-order sorption kinetic constant. The high correlation coefficients indicated that Tl(I) uptake onto both materials can be well represented by the pseudo-first-order model. It was worth mentioning that the loading of nanosized HMO hardly imposes any negative effect on kinetics, though HMO encapsulation would cause considerable pore blockage. Similar kinetic behavior was also observed for lead ion removal by polymer-based zirconium phosphate [36], and Donnan membrane effect resulting from D001 is expected to favor sorption kinetics through permeation enhancement [19, 21]. Of note, HMO-001 does not exhibit higher capacity than D001 in the same dosage in mass. It is not surprising because HMO loadings within D001 would increase the density of the spherical beads. For the same mass dosage of both adsorbents, a less

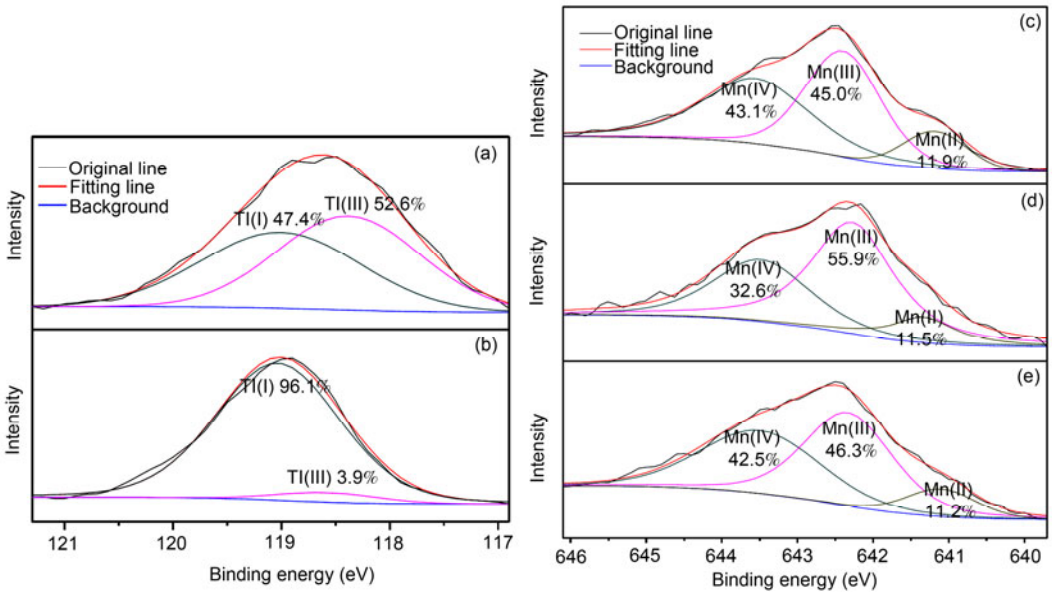

Figure 5 XPS spectra of Tl 4f7/2 and Mn 2p3/2 core levels of the HMO-001 samples (a) after Tl(I) adsorption at pH 2.2; (b) after Tl(I) adsorption at pH 5.8; (c) the fresh one; (d) after Tl(I) adsorption at pH 2.2; (e) after Tl(I) adsorption at pH 5.8. Note that 4f7/2 values of Tl(I) (190.05 eV) and Tl(III) (189.50 eV) are available by detecting the sample of $TiNO_3$ and Tl_2O_3, respectively, while those of Mn species are available from [33], i.e., 641.1, 642.3, and 643.6 eV for Mn(II), Mn(III), and Mn(IV), respectively.

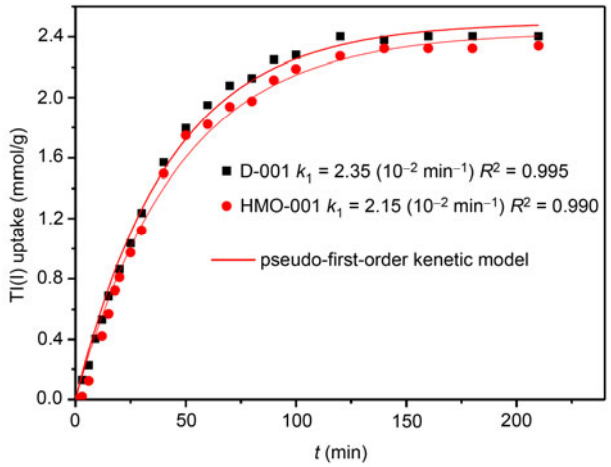

Figure 6 Adsorption kinetics of Tl(I) ion onto D-001 and HMO-001 at 298 K and pH 5.8. S/L ratio =1.00 g/L, initial Tl(I) 0.50 mmol/L.

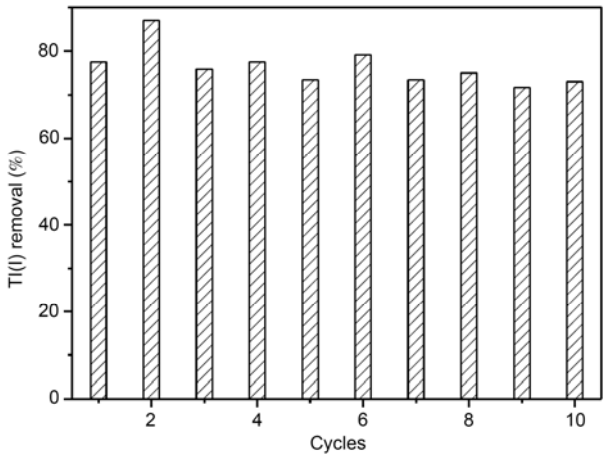

Figure 7 Batch cyclic adsorption-regeneration results of HMO-001 at 298 K. Sorption: S/L = 1.00 g/L, initial Tl(I) 0.30 mmol/L and Ca(II) 5 mmol/L, pH 5.8; Regeneration: 5 mL NaOH-NaOCl solution as the regenerant.

amount of D001 was contained in HMO-001 as compared to D001, resulting in its lower capacity of HMO-001, even though HMO also exhibited metal adsorption. However, it does not matter because for practical application, generally it is not adsorption capacity but adsorption preference to determine the applicability of a given adsorbent for trace Tl removal, because other competing cations were present as much greater levels than the target Tl(l) species.

3.6 Batch adsorption-regeneration cycles

The exhausted HMO-001 was subjected to regeneration by using NaOH-NaClO binary solution (alkalinity at 7.8% and active chlorine at 5.0%) as the regenerant. As depicted in Figure 7, after treatment by the binary solution, HMO-001 can be repeatedly used for at least 10 cycles without any significant efficiency loss. To further demonstrate the regeneration efficiency of the binary solution, we just employed the deionized water instead to rinse the exhausted HMO-001 beads for cyclic runs, keeping other conditions identical. For water-rinsing based cyclic runs, Tl(I) removal decreased dramatically to 34.2% for the second cycle and 0.8% for the third cycle. The comparative study demonstrated the efficiency of NaOH-NaClO binary solution for regeneration of Tl(l)-preloaded composite.

Interestingly, negligible Tl was detected in the NaOH-

NaOCl solution after regeneration, indicating that all the adsorbed Tl still remained in the HMO-001 after regeneration. To confirm the result we analyzed Tl amount of the HMO-001 particles at the end of the cyclic runs. Totally, the adsorbed amount of Tl(I) after cyclic runs is 45.8 mg, while that in the composite beads is 44.5 mg, that is, about 97.2% of the adsorbed Tl(I) remained in the adsorbent. Such interesting phenomena may be explained by the assumption that the adsorbed Tl(I) was oxidized into Tl(III) by NaOCl and deposited as insoluble $Tl(OH)_3$ or Tl_2O_3 within HMO-001, resulting in the Tl(I)-occupied sites of HMO released for next-cycle adsorption. XPS analysis on the oxidized HMO-001 samples preloaded with Tl(I) demonstrated that all the Tl compounds inside the sample were Tl(III) species, because we did not get any Tl(I) signals in the sample. In addition, with the increasing cycles the deposition of $Tl(OH)_3$ or Tl_2O_3 would possibly affect the structure and capacity of HMO-001. How to further treat the completely exhausted HMO-001 may be a question to be solved. We suggested that the exhausted HMO-001 be rinsed by acidic solution (HCl or H_2SO_4) to recover the host D-001 because the encapsulated HMO was leachable at acidic pH, and, according to the research by Bidoglio *et al*. [32], the concentrated Tl-Mn effluent could be readily neutralized by alkaline to chemically deposit Tl(III) species. Additional work is still required to examine the applicability of the process.

3.7 Column adsorption

The effluent history of fixed-bed columns packed with HMO-001 or D-001 was illustrated in Figure 8, where a synthetic Tl(I)-contained solution, Tl(l)-contaminated industrial effluent, and natural water was employed as the feeding solution respectively. As shown in Figure 8(a), for the synthetic solution, Tl(I) broke through shortly from the D-001 column only after ~50 bed volumes (BV), while the HMO-001 column had a valid volume of 1000 BV before the Tl(I) concentration exceeded 140 μg/L, the MCL of industrial effluent recommended by EPA. The results are consistent with the preferable sequence of both materials as discussed earlier. C_e/C_0 in excess of unity on the breakthrough curve of D-001 could be reasonably explained by the elution effect of the competing ions [37]. In other words, a fraction of Tl(I) initially loaded on D-001 could be jostled by the competing ions when insufficient adsorption sites were available. Nevertheless, similar phenomenon was not observed for HMO-001 because of the improved selectivity of the nanocomposite. To further examine the feasibility of HMO-001 for practical application, we employed an industrial effluent as the feeding solution. Results in Figure 8(b) suggested that the effective volume per run is around 1800 BV for the industrial effluent. Besides, HMO-001 can serve as an effective material to remove trace Tl(I) to a safer lev-

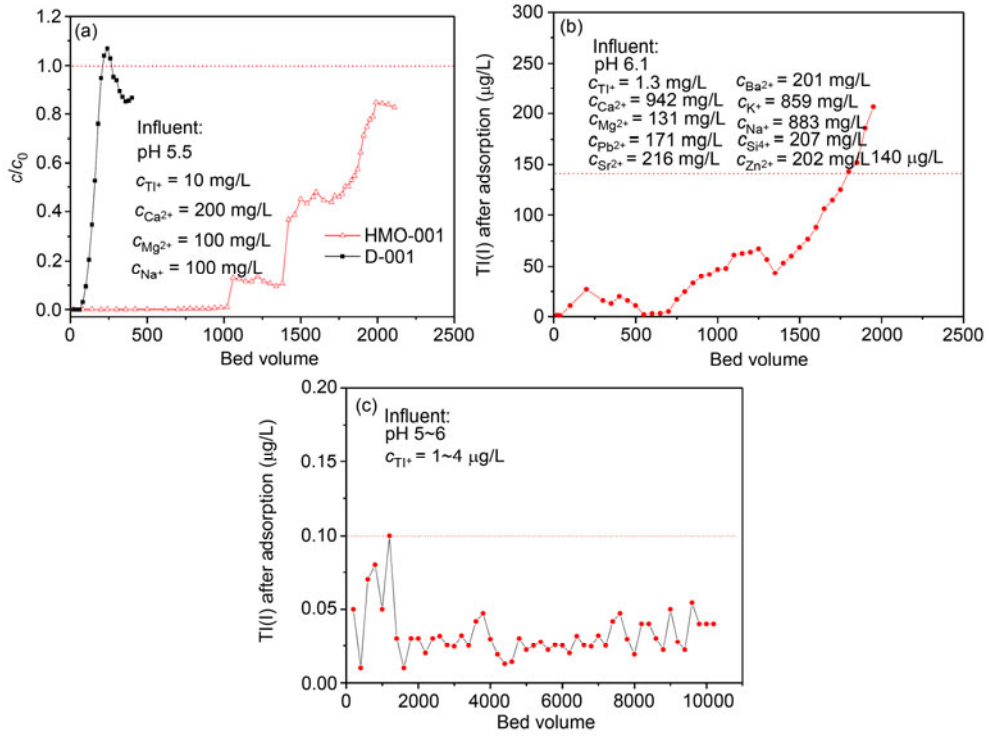

Figure 8 Breakthrough curves of Tl(I) from synthetic solution and really contaminated waters by HMO-001 at 298 K. Feeding solution (a) a synthetic solution in the presence of other co-ions, D-001 column was employed for reference; (b) an ore-mining effluent after activated alum precipitation was sampled in Guangdong Province (China) as the feeding solution; (c) natural river waters near an ore-mining plant in Guangdong Province were sampled as the feeding solution. The superficial liquid velocity (SLV) and the empty bed contact time (EBCT) are 1.50 m/h and 6.0 min for (a) and (b), and 3.0 m/h and 3.0 min for (c).

el. As illustrated in Figure 8(c), HMO-001 can reduce Tl(I) in natural water from 1–4 μg/L to lower than 0.1 μg/L, the MCL in drinking water regulated by Ministry of Health of China, with the treatable volume more than 10000 BV. Of note, Mn concentration in the industrial effluent and natural water after adsorption was 0.08–0.11 mg/L and < 0.05 mg/L, much lower than the standard for discharged wastewater quality (< 2 mg/L) and drinking water (< 0.1 mg/L) in China. Also, the result is consistent with the fact that no HMO leaching was detected from HMO-001 at pH higher than 3 (Figure 2).

4 Conclusions

The experimental results proved that the nanocomposite HMO-001 is a promising material for highly efficient removal of thallium from contaminated waters of varying chemistry in terms of both adsorption capacity and adsorption selectivity. Another attractive option is that the exhausted HMO-001 can be readily regenerated for at least 10-cycle use without any significant capacity loss. Considering the limitations of laboratory-scale experiments and the complexities of actual thallium pollution, further study is required to evaluate the feasibility of HMO-001 for practical application.

The study was financially supported by the National Natural Science Foundation of China (51078179), Natural Science Foundation of Jiangsu Province (BK2012017/2011016), State Key Scientific Project for Water Pollution Control and Treatment (2012ZX07206003), and Program for New Century Excellent Talents in University of China (NCET10-0490).

1 Delvalls TA, Saenz V, Arias AM, Blasco J. Thallium in the marine environment: First ecotoxicological assessments in the Guadalquivir estuary and its potential adverse effect on the Donana European natural reserve after the Aznalcollar mining spill. *Ciencias Marinas*, 1999 25: 161–175
2 Kazantzis G. Thallium in the environment and health effects. *Environ Geochem Health*, 2000, 22: 275–280
3 Peter ALJ, Viraraghavan T. Thallium: A review of public health and environmental concerns. *Environ Int*, 2005, 31: 493–501
4 Casiot C, Egal M, Bruneel O, Verma N, Parmentier M, Elbaz-Poulichet F. Predominance of aqueous Tl(I) species in the river system downstream from the abandoned Carnoules mine (Southern France). *Environ Sci Technol*, 2011, 45: 2056–2064
5 Xiong YL. The aqueous geochemistry of thallium: Speciation and solubility of thallium in low temperature systems. *Environ Chem*, 2009, 6: 441–451
6 Zitko V. Toxicity and pollution potential of thallium. *Sci Total Environ*, 1975, 4: 185–192
7 Seiler HG, Sigel H, Sigel A. *Handbook on Toxicity of Inorganic Compounds*. New York: Marcel Dekker Inc., 1989
8 Cheam V. Thallium contamination of water in Canada. *Water Qual Res J Can*, 2001, 36*:* 851–878
9 Kazantzis G. *Thallium Handbook on the Toxicology of Metals*. Amersterdam: Elsevier Science, 1986. 549–567
10 Leonard A, Gerber GB. Mutagenicity, carcinogenicity and teratogenicity of thallium compounds. *Mutat Res-Rev Mutat*, 1997, 387: 47–53
11 Zhang Z, Zhang BG, Long JP, Zhang XM, Chen GL. Thallium pollution associated with mining of thallium deposits. *Sci China, Ser D*, 1998, 41: 75–81
12 US EPA (Environmental Protection Agency). Technical factsheet on: Thallium. http://www.epa.gov/safewater/dwh/t-ioc/thallium. html, 2002
13 China MH (Ministry of Health). Standard for drinking water quality. GB5749-2006, 2006
14 Xiao TF, Boyle D, Guha J, Rouleau A, Hong YT, Zheng BS. Groundwater-related thallium transfer processes and their impacts on the ecosystem: Southwest Guizhou Province, China. *Appl Geochem*, 2003, 18: 675–691
15 Zhang L, Huang T, Zhang M, Guo XJ, Yuan Z. Studies on the capability and behavior of adsorption of thallium on nano-Al_2O_3. *J Hazard Mater*, 2008, 157: 352–357
16 Senol ZM, Ulusoy U. Thallium adsorption onto polyacryamide- aluminosilicate composites: A Tl isotope tracer study. *Chem Eng J*, 2010, 162: 97–162
17 Yantasee W, Warner C, Sangvanich T, Addleman RS, Carter TM, Wiacek RJ, Fryxell GE, Timchalk C, Warner MG. Removal of heavy metals from aqueous systems with thiol functionalized superparamagnetic nanoparticles. *Environ Sci Technol*, 2007, 41: 5114–5119
18 Sangvanich T, Sukwarotwat V, Wiacek RJ, Grudzien RM, Fryxell GE, Addleman RS, Timchalk C, Yantasee W. Selective capture of cesium and thallium from natural waters and simulated wastes with copper ferrocyanide functionalized mesoporous silica. *J Hazard Mater*, 2010, 182: 225–231
19 Cumbal L, SenGupta AK. Arsenic removal using polymer-supported hydrated iron(III) oxide nanoparticles: Role of Donnan membrane effect. *Environ Sci Technol*, 2005, 39: 6508–6515
20 Pan BJ, Wu J, Pan BC, Lv L, Zhang WM, Xiao LL, Wang XS, Tao XS, Zheng SR. Development of polymer-based nanosized hydrated ferric oxides (HFOs) for enhanced phosphate removal from waste effluents. *Water Res*, 2009, 43: 4421–4429
21 Sarkar S, SenGupta AK. The Donnan membrane principle: Opportunities for sustainable engineered processes and materials. *Environ Sci Technol*, 2010, 44: 1161–1166
22 Zhao X, Lv L, Pan BC, Zhang WM. Polymer-supported nanocomposites for environmental application: A review. *Chem Eng J*, 2011, 170: 381–394
23 Zhang QR, Pan BC, Zhang WM, Pan BJ, Jia K, Zhang QX. Selective sorption of lead, cadmium, and zinc ions by a polymeric cation exchanger containing nano-$Zr(HPO_3S)_2$. *Environ Sci Technol*, 2008, 42: 4140–4145
24 Parida KM, Kanungo SB, Sant BR. Studies on MnO_2. 1. Chemical composition, microstructure and other characteristics of some synthetic MnO_2 of various crystalline modifications. *Electrochimica Acta*, 1981, 26: 435–443
25 Pan BC, Su Q, Zhang WM, Zhang QX, Ren HQ, Zhang QR. A process to prepare a hybrid sorbent by impregnating hydrous manganese dioxide (HMO) nanoparticles within polymer for enhanced removal of heavy metals. Chinese Patent, 200710134050.9, 2007
26 Lowry GV, Johnson KM. Congener-specific dechlorination of dissolved PCBs by microscale and nanoscale zerovalent iron in a water/methanol solution. *Environ Sci Technol*, 2004, 38: 5208–5216
27 Yavuz CT, Mayo JT, Yu WW, Prakash A, Falkner JC, Yean S, Cong L, Shipley HJ, Kan A, Tomson M, Natelson D, Colvin VL. Low-field magnetic separation of monodisperse Fe_3O_4 nanoparticles. *Science*, 2006, 314: 964–967
28 Lafferty BJ, Ginder-Vogel M, Zhu MQ, Livi KJT, Sparks DL. Arsenite oxidation by a poorly crystalline manganese-oxide. 2. Results from X-ray absorption spectroscopy and X-ray diffraction. *Environ Sci Technol*, 2010, 44: 8467–8472
29 Misono M, Ochiai E, Saito Y, Yoneda Y. A new dual parameter scale for the strength of Lewis acids and bases with the evaluation of their softness. *J Inorg Nucl Chem*, 1967, 29: 2685–2691

30 Dahal MP, Lawrance GA. Adsorption of thallium(I), lead(II), copper(II), bismuth(III) and chromium(III) by electrolytic manganese dioxide. *Adsorp Sci Technol*, 1996, 13: 231–240
31 Xu Y, Boonfueng T, Axe L, Maeng S, Tyson T. Surface complexation of Pb(II) on amorphous iron oxide and manganese oxide: Spectroscopic and time studies. *J Colloid Interface Sci*, 2006, 299: 28–40
32 Bidoglio G, Gibson PN, Ogorman M, Roberts KJ. X-ray absorption spectroscopy investigation of surface redox transformations of thallium and chromium on colloidal mineral oxides. *Geochim Cosmochim Acta*, 1993, 57: 2389–2394
33 Lin KD, Liu WP, Gan J. Oxidative removal of bisphenol A by manganese dioxide: Efficacy, products, and pathways. *Environ Sci Technol*, 2009, 43: 3860–3864
34 Stumm W, Morgan JJ. *Aquatic Chemistry*. 3rd Ed. New York: Wiley, 1996
35 Dogan M, Abak H, Alkan M. Adsorption of methylene blue onto hazelnut shell: Kinetics mechanism and activation parameters. *J Hazard Mater*, 2009, 164: 172–181
36 Pan BC, Zhang QR, Zhang WM, Pan BJ, Du W, Lv L, Zhang QJ, Xu ZW, Zhang QX. Highly effective removal of heavy metals by polymer-based zirconium phosphate. A case study of lead ion. *J Colloid Interface Sci*, 2007, 310: 99–105
37 Pan BC, Zhang QX, Meng FW, Li XT, Zhang X, Zheng JZ, Zhang WM, Pan BJ, Chen JL. Sorption enhancement of aromatic sulfonates onto an aminated hyper-cross-linked polymer. *Environ Sci Technol*, 2005, 39: 3308–3313